Evaluation of Moisture Transport Properties Based on Modelling of Silane-based Impregnation Agent Effects on Concrete Surface Layer

Yuya Takahashi*, *Ayaka* Miyake, *Motohiro* Ohno, and *Tetsuya* Ishida

Department of Civil Engineering, School of Engineering, The University of Tokyo, Hongo 7-3-1, Bunkyo-Ku, Tokyo 113-8656, Japan

Abstract. It is now desirable to establish a technique for long-term prediction of the effects of silane-based impregnation agent on concrete structures exposed to various environments. To meet this requirement, the purpose of this study is set to establish the model to evaluate the effect of a silane-based impregnation agent on the waterproofing properties of cementitious materials based on microscopic mechanisms. Several mortar specimens were prepared with the silane-based impregnation agent, and moisture absorption and evaporation experiments were conducted. The results showed that the application of the agent was shown to effectively inhibit the penetration of moisture into the interior of the cementitious materials. The effect of the silane-based impregnation agent was modeled in a multiscale pore structure model by applying a microscopic water-repellent effect to the pores in which no pore water was present at the time of agent coating. The analysis with proposed model showed that, as in the experiment, the moisture supply was reduced by the application of the agent, whereas the amount of moisture loss remained almost the same with and without the agent. Moreover, the analysis quantitatively showed that the water content can continue to decrease with silane treatments, even under repeated wet-dry conditions.

1 Introduction

Water supply is a key factor that causes material in concrete structures to deteriorate through mechanisms such as steel corrosion [1], alkali-silica reaction [2], and frost damage [3]. One possible method to make concrete structures more durable is to reduce water ingress into the concrete. Many surface treatment techniques based on this approach, such as the use of surface impregnation materials to reduce water ingress, have been developed [4,5]. Surface impregnation agents have many advantages, such as their easy and fast installation, relatively low cost, and capacity for visual inspection even after installation, as they can be applied without changing their appearance. This study focuses on a silane-based impregnation agent [4]. Silane-based impregnation agents reduce the water permeability by forming a water-repellent layer within the concrete surface [6]. The advantage of the silane-based

* Corresponding author: katahashi@concrete.t.u-tokyo.ac.jp.

impregnation agent is that it does not inhibit moisture evaporation, allowing the interior to remain drier, whereas the surface covering material prevents moisture from evaporation from the interior, causing moisture to accumulate inside the material. To discuss the effect of silane-based impregnation agents on the long-term durability of concrete structures, experimental investigations and simulation-based approaches are necessary. The authors have been developing a multiscale thermodynamic analytical system [7] that considers the cement hydration process, pore structure development, and water transport/equilibrium in pore structures, and is expected to be utilized to simulate the effect of silane-based impregnation agents based on microscopic phenomena.

In this study, we propose a method to consider the effect of a silane-based impregnation agent in a simulation. Then, based on the experimental results, the effects of the impregnation agent on the water flux at the surface layer of the concrete is studied for different states of water and flux directions. The measurement results are used to evaluate the performance of the proposed model. The capability of evaluating the long-term durability performance of concrete through simulations is also discussed.

2 Model Consideration of Silane-Based Imprenation Agent

This study utilized a multiscale thermodynamic analytical system called DuCOM [7], which is a finite element (FE) system developed by the authors, for the simulations. Figure 1 shows the overall scheme for calculating the combined process of cement hydration, pore structure development, and moisture state.

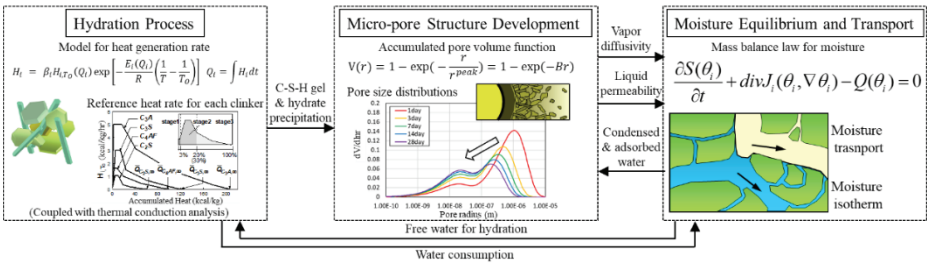

Fig. 1. Overall calculation scheme of thermodynamic analytical system [7]

Considering the hydration heat of each clinker, the hydrate precipitation was calculated, which was reflected in the calculation of pore size distributions. The moisture content and moisture transfer inside the concrete were calculated in the moisture equilibrium and transport model, which considers water consumption from the hydration model and the developed micropore structure. In the moisture equilibrium and transport model, given the vapor pressure P (Pa) at each position with unsaturation in the cement paste, the liquid-vapor interface radius r_c (m) can be obtained as follows:

$$r_c = C \cdot r_s = -\frac{2C \cdot \gamma \cdot M}{\rho \cdot RT} \frac{1}{\ln\left(\frac{P}{P_0}\right)}, C = 2.15 \quad (1)$$

where C is the coefficient representing the thickness of the adsorbed water layer on the pore wall, r_s is the pore radius (m) calculated from Kelvin's equation, γ is surface tension of the water (N/m), M is the molar mass of water (kg/mol), ρ is the density of water (kg/m^3), R is the universal gas constant (J/mol/K), T is the absolute temperature (K), and P_0 is the saturated vapor pressure (Pa). Using the liquid-vapor interface radius r_c, the saturation degree S, liquid water flux q_l, and water vapor flux q_v in the cement paste are expressed by the following equations [7]:

$$S = \int_0^{r_c} \Omega \, dr \tag{2}$$

$$q_l = -\frac{\rho \phi^2}{50\eta} \left(\int_0^{r_c} r dV \right)^2 \nabla P \tag{3}$$

$$q_v = \frac{\rho_s \phi D_0}{(\pi/2)^2} \int_{r_c}^{\infty} \frac{dV}{1+N_k} \left(\frac{Mh}{\rho RT} \right)^2 \nabla P \tag{4}$$

where Ω (= *dV/dr*) is the pore size distribution function, f is porosity, η is the viscosity of water (Pa·s), ρ_s is the density of saturated vapor (kg/m^3), D_0 is the self-diffusion coefficient of water vapor, N_k is the Knudsen number, and h is relative humidity (RH) (= P/P_0). In Eqs. 2, 3, and 4, the liquid-vapor interface radius r_c is set to the upper or lower limit of the integral range; thus, it can be considered that the voids with sizes below of r_c are filled with liquid water in the pore size distributions, and the saturated and dried pore areas are considered in the liquid water flux and vapor flux, respectively.

Considering the effect of the silane-based impregnation agent, the contact angle between the water and pore wall in the pore space where the impregnation agent was applied was more than 90°, and no meniscus could be formed (Fig. 2) [6]. In other words, the pore space where the impregnation agent was applied was in a state in which it was difficult for water to remain because of the water-repellent effect. Therefore, in this study, it was assumed that the impregnation material was applied to all dried pore spaces with sizes above r_c when the surface impregnation work was conducted; thereafter, no water could exist in the area (Fig. 2). In this model, the values of r_c in Eqs. 2, 3, and 4 were calculated using Eq. 5:

$$r_c = \begin{cases} r_c \ (when \ P < P_{im}) \\ r_{c_{im}} (when \ P \geq P_{im}) \end{cases} \tag{5}$$

where P_{im} is the vapor pressure when the impregnation work is conducted, and r_{c_im} is the corresponding liquid-vapor interface radius, which is a constant value in the succeeding time steps in the simulation. For the portions of the surface layer affected by the impregnation agent, this consideration was applied, so that the effect of the surface impregnation agent could be properly considered.

With this consideration, even when the pore water pressure increased, the pores remained unsaturated, the liquid water permeability remained low, and the vapor conductivity remained high.

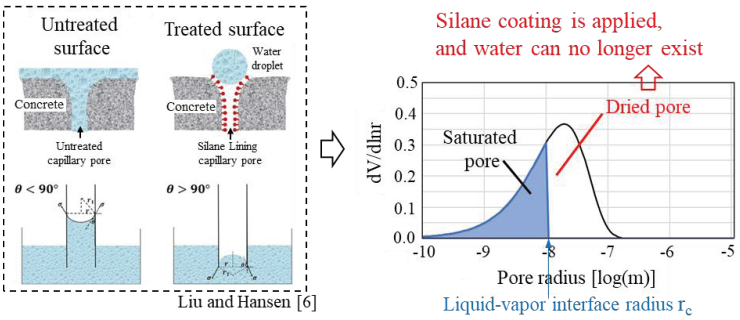

Fig. 2. Consideration of silane coating effect on water saturation model.

3 Experiment On Water Transport in Mortar

Experiments were conducted to obtain the data for model validation. The mortar was cast with the mix proportions listed in Table 1 and subjected to several water flux experiments, as explained in Table 2 ((i) water absorption, (ii) moisture absorption, and (iii) moisture

dissipation tests), which were planned with reference to the guidelines provided by the Japan Society of Civil Engineers [8]. Ordinary Portland cement with a density of 3.15 g/cm^3 was used, and sandstone with a density of 2.59 g/cm^3 was used as the fine aggregate. First, the mortar was cast into 100 × 100 × 400 mm rectangular prism shapes, and after 1 day of sealing and 6 days of water curing, each sample was cut using a wet concrete cutter into the appropriate specimen size for each experiment. After cutting, specimens are exposed to constant 20 °C and 60% RH conditions (air curing). Epoxy coating was applied to the side surfaces of the specimens four days before the silane treatment. For silane treatments, a silane-siloxane-based surface impregnation agent (Aqua Seal 1400, DAIDO corporation) was applied to the specimens using brushes, as shown in Fig. 3(a). After silane treatment, the specimens were kept at 20 °C and RH 60% until the start of the tests. Three specimens were fabricated for each case.

For the (i) water absorption test, 100 × 100 × 100 mm cube specimens cut from 100 × 100 × 400 mm prism mortar samples were used. To ignore the effect of position within the 100 × 100 × 400 mm prism, the tip part of the prism was removed, as shown in Fig. 3(b). Epoxy coating on four side surfaces and silane coating on the two other surfaces were applied (for only half of the specimens) at 31 and 35 days of material age, respectively. After 14 days of air curing, the specimens were immersed in water while maintaining a water level 20 mm higher than the tops of the specimens. Water was absorbed from two opposite surfaces of the specimens and the weight changes of the specimens were recorded.

For the (ii) moisture absorption and (iii) moisture dissipation tests, 20 × 100 × 100 mm specimens were cut from a 100 × 100 × 100 mm cube (as shown in Fig. 3(c)), and epoxy coating on four side surfaces and silane coating on one 20 × 100 mm face were applied (for only half of the specimens) at 34 and 38 days of material age, respectively. In the (ii) moisture absorption test, after 17 days of air curing, one remaining surface was coated with tight adhesive tape, and the specimens were placed above the water, which was kept at the bottom inside the desiccators. This implies that humid conditions can cause moisture absorption from the outside to the inside of the specimens. In the (iii) moisture dissipation test, after 14 days of air curing, the non-coated surface was placed into the water, and water was absorbed from the opposite surface of the silane treatment for 3 days. After that, the bottom surface was tightly coated by adhesive tape, and the specimens were kept in 15 °C and RH 78% conditions, under which the moisture could evaporate from the top surface of the specimens. In each test, weight changes were recorded, and the moisture flux from the surface was calculated.

Table 1. Mix proportions.

W/C (%)	Unit weight (kg/m^3)		
	Water	**Cement**	**Fine aggregate**
48.5	273	562	1235

Table 2. Experimental conditions.

	(i) Water absorption	**(ii) Moisture absorption**	**(iii) Moisture dissipation**
State of water	Liquid water	Vapor	Vapor
Flux direction	Inward	Inward	Outward
Specimen size	100 × 100 × 100 mm	20 × 100 × 100 mm	20 × 100 × 100 mm
Coating time	Day 35	Day 38	Day 38
Experimental condition	7 days of water immersion	40 days of humid condition	3 days of water absorption from bottom surface →40 days of drying from top
Measurement	Weight change	Weight change	Weight change

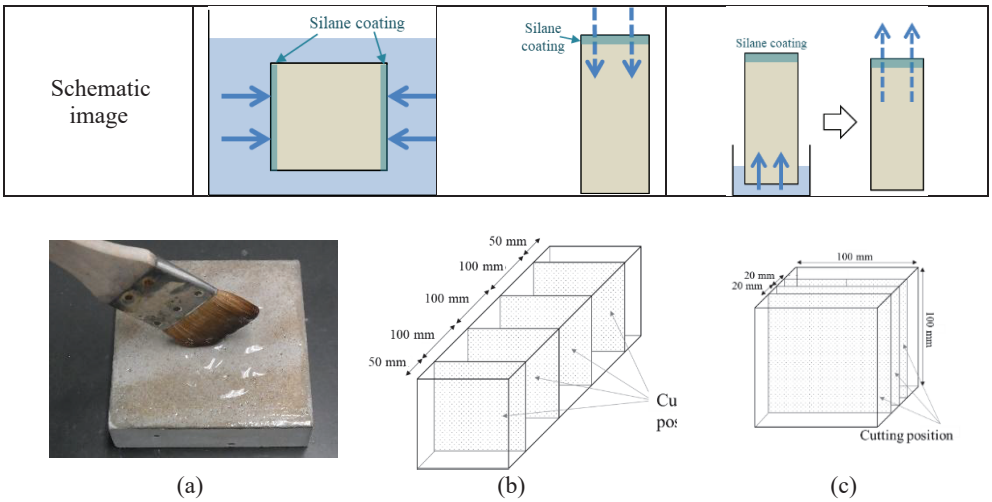

Fig. 3. Specimen preparation, (a) Silane coating with brush, (b) 100 cm cube cutting, (c) 20 cm thickness slicing.

Figure 4 shows the measured weight change (water absorption) with and without silane treatment in the (i) water absorption test. The average values of 3 specimens were plotted for each case. Compared to the specimens without the silane impregnation agent treatment, significantly lower water absorption was observed in the silane-treated specimens in this study, which is similar to the results of many previous studies [6,9]. Because of the limited water permeability of the surface layer of the specimens caused by the silane impregnation agent, the water flux from the outside to the inside was significantly reduced.

Figures 5 and 6 show the moisture fluxes measured in the (ii) moisture absorption and (iii) moisture dissipation tests, respectively. The measured weight change was divided by the area of the test surface to calculate the moisture flux. In the moisture absorption test (Fig. 5), the specimen with silane had a lower moisture flux than the specimens without silane, whereas the ratio of the reduction in water absorption was smaller than that in the liquid water absorption test (Fig. 4). The reduction ratio of the flux appears to differ depending on the state of the water. Moreover, the moisture dissipation test results (Fig. 6) showed that the specimens with silane had almost the same moisture flux as the specimens without silane. Even when silane treatment was applied, the drying speed of the specimen did not change, which is beneficial for maintaining a low water content inside cementitious materials over the long term. In summary, inward liquid and moisture transport in mortar were reduced by silane treatment, which is the same tendency from the previous research [6,9], whereas outward moisture transport in the mortar did not change with or without silane treatment. The characteristic water flux behaviors resulting from the application of the silane impregnation agent were reproduced in the simulations in the next section.

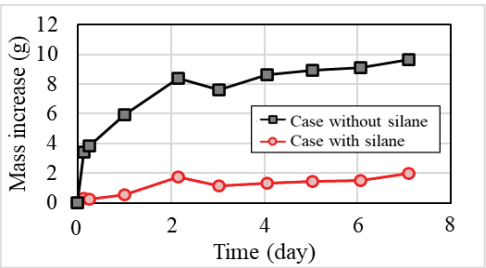

Fig. 4. Measured weight change in water absorption test.

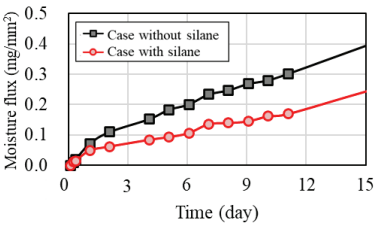

Fig. 5. Measured flux in moisture absorption test.

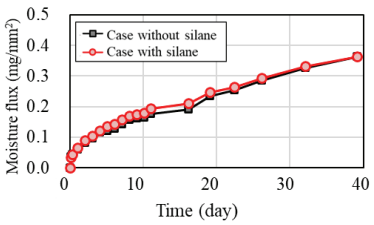

Fig. 6. Measured flux in moisture dissipation test.

4 Simulations by proposed model consideration

First, the simple 1D simulations were conducted to verify the implemented model consideration. One-dimensional FE mesh with 100 mm length was prepared and the mix proportion shown in Table 1 was set. After 4- day sealed curing, the surface elements were exposed to 20 °C and RH 55% condition until 55 days, after that, exposed to 20 °C and RH 99.9% condition. For the case with silane, the proposed silane model consideration was applied on the surface 2 mm elements at 7 days of material age. Figure 7 shows the transitions of simulated total water contents of whole elements, and Fig. 8 shows the distributions of water content with and without silane treatment. We can see that the decrease of water content during drying phase is totally the same with and without silane, while the increase of water during wetting phase is largely suppressed in the case with silane (Figs. 7 and 8). This is due to the suppressed water content at the surface 2 mm layer with silane model applied (Fig. 8(b)), as expected.

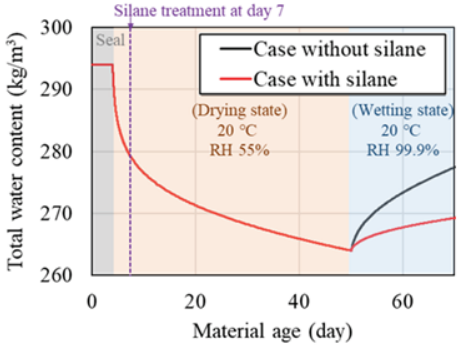

Fig. 7. Transitions of simulated total water content,

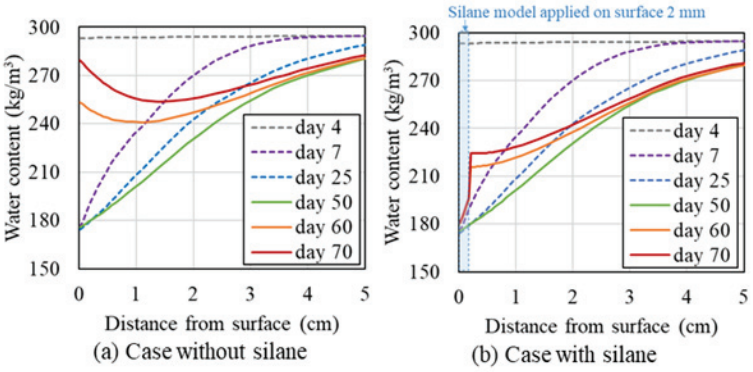

Fig 8. Distribution of water content at several material age

Then, reproduction analyses were conducted to validate the proposed model (Fig. 2). Three-dimensional FE meshes were prepared as shown in Fig. 9, the mix proportions are shown in Table 1, and the same process was set for each experiment. At the time of silane coating, the consideration proposed in Eq. 5 was applied to the surface element layers and r_{c_lim} was considered in the following processes. Based on previous studies, the depth of silane impregnation was assumed to be 6 mm [9].

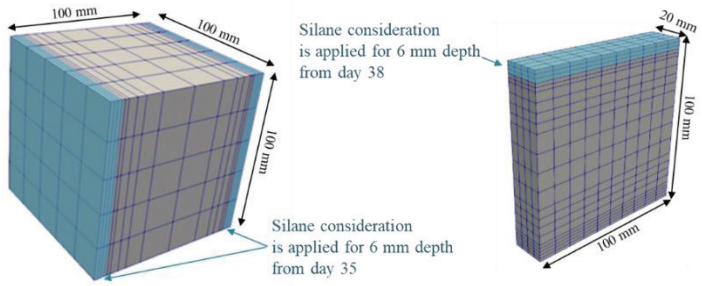

Fig. 9. Prepared analytical meshes for simulation studies.

Figure 10 shows the simulated mass increase during the water absorption process for the (i) water absorption test. Similar to the results of the experiment (Fig. 4), the mass increase in the case of silane treatment was approximately 80% less than in the case without silane treatment. In the case of silane treatment, the water content in the surface element layers (6 mm depth) cannot increase when the calculated vapor pressure P becomes higher than P_{im} because the upper bound of the liquid-vapor interface radius is limited to the value r_{c_im}, as shown in Eq. 5. Therefore, the liquid water flux calculated using Eq. 3 is kept small, which prevents a mass increase even when liquid water pressure is applied to the surfaces of the elements.

Figures 11 and 12 show the simulated moisture flux for the (ii) moisture absorption and (iii) moisture dissipation tests. In the simulation of (ii), the moisture absorption test (Fig. 11), the reduction in moisture flux due to the silane treatment measured in the experiment (Fig. 5) was effectively reproduced. Note that both the liquid water flux and the vapor flux are reduced with silane treatment (both in the experiment and simulation) when the direction of the flux is inward (wetting process). The vapor permeability (the right term without ∇P in Eq. 4) remained large because of the limited r_c value (r_{c_im}), but the water content (calculated using Eq.3) of the silane-impregnated layer was also limited, which prevented moisture flux in the wetting process. Different reduction ratios owing to different water states (liquid or vapor) were reproduced well.

In the simulation of (iii) the moisture dissipation test (Fig. 12), the moisture flux was almost the same between the cases with and without silane treatment, which is the same behavior as in the experiments (Fig. 6). In this drying process, the vapor permeability remained high, and the calculated water content was lower than in than the condition corresponding to r_{c_im}. The calculated vapor pressure P is always smaller than the threshold value P_{im}; therefore, the moisture flux calculation did not change between the cases with and without silane treatment. Thus, from a microscopic viewpoint, the effect of the silane impregnation agent on the surface layer of the cementitious materials can be effectively understood and reproduced.

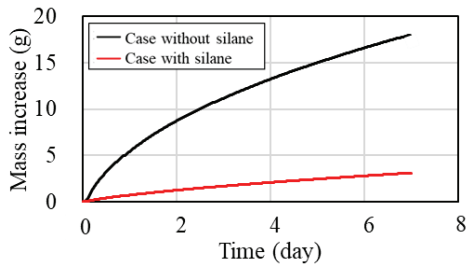

Fig. 10. Simulated weight change for water absorption test.

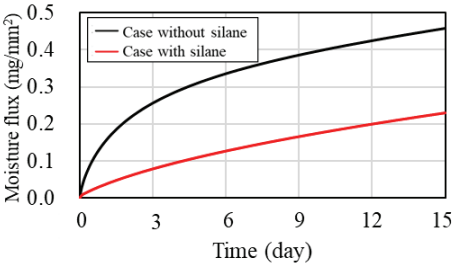

Fig. 11. Simulated flux for moisture absorption test.

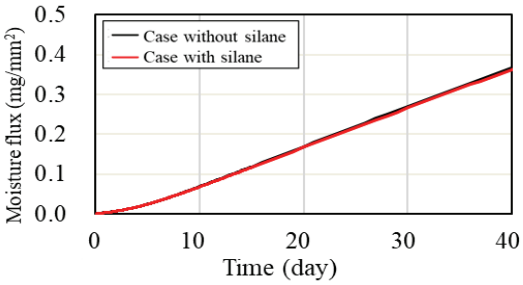

Fig. 12. Simulated flux for moisture dissipation test.

Using the validated model, a comparative study of wet-dry cycles was conducted to investigate the long-term behavior of moisture conditions in cementitious materials. One dimensional analytical mesh with a length of 100 mm was prepared, and the same mix proportions were used as input. After 1 day of sealing, surface was exposed to 20 °C and 60% RH conditions, and silane treatment was applied to the 2 mm surface element layers at day 21. From 50 days of material age, wet-dry cycles were set with both wetting (RH 99.9%) and drying (RH 60.0%) periods of 1 week.

Figure 13 shows the water content calculated throughout the simulations. During the first drying period (until 50 days), the cases with and without silane treatment had the same decrease in water content, after which wet-dry cycles started. In the case without silane treatment, the total water content gradually increased during the wet-dry cycles, because the wetting speed is generally larger than the drying speed in cementitious materials [10]. On the other hand, interestingly, the water content decreased even in wet-dry cycles in the case with silane treatment. The speed of liquid water ingress during the wetting period was significantly reduced (as shown in Fig. 10) and was even lower than the water evaporation speed during the drying period. As a result, the water content continues to decrease during the wet-dry cycles. Therefore, the significant effects of the silane impregnation agent in reducing water content and enhancing the long-term durability of concrete structures were successfully demonstrated.

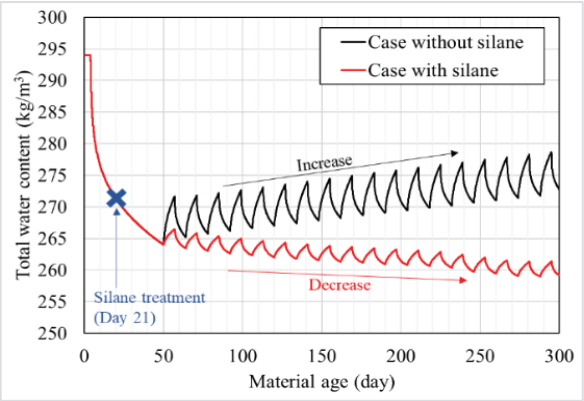

Fig.13. Simulated water content during wet-dry repetition.

Finally, the effect of the impregnation depth was numerically studied. The silane treatment model was applied at different depths from the surface (2, 4, and 6 mm) to simulate the (ii) moisture absorption test. Figure 14 shows the simulated moisture fluxes at different silane impregnation depths. A large decrease in the moisture flux compared to the case without silane was observed with a larger silane layer depth. The reduction in the moisture flux was almost halved when the impregnation depth was reduced from 6 to 2 mm. The depth of impregnation should be appropriately set to predict the behavior of the materials. Previous studies [9,11] have shown that the impregnation depth can change with various factors, such as the water-to-cement ratio, dosage of the agent, and drying state of the concrete. In the future, a reasonable process for predicting the impregnation depth should be discussed and implemented in a simulation system for the long-term performance evaluation of various types of concrete structures.

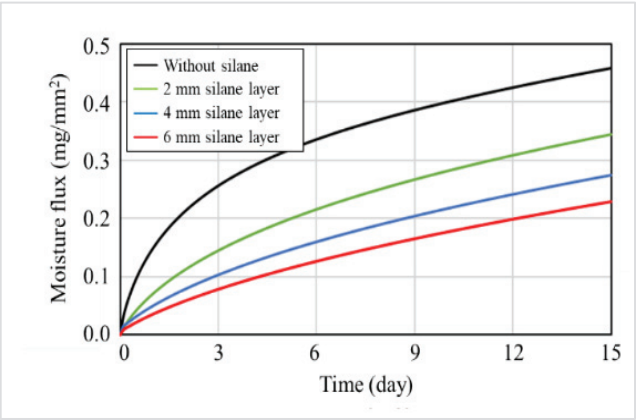

Fig. 14. Moisture absorption with different silane impregnation depth.

5 Conclusion

In this study, the effects of a silane-based impregnation agent on the water transport properties at the surface layers of cementitious materials were investigated. Considering the microscopic water-repellent properties at the pore wall, a method was proposed to consider the effect of the silane-based impregnation agent on the existing micropore structure model. Then, several mortar specimens were prepared, with and without silane treatment, and water

absorption, moisture absorption, and moisture evaporation experiments were conducted. The results showed that the liquid water and vapor absorption were significantly reduced by the silane-based impregnation agent, whereas the vapor evaporation process remained unchanged. These characteristic behaviors involving the silane-based impregnation agent were well reproduced in simulations using the proposed method to consider the microscopic effects of the silane-based impregnation agent. Thus, the mechanisms for reducing the water content inside concrete with a silane-based impregnation agent were quantitatively demonstrated based on microscopic phenomena. It was also shown that the water content could continue to decrease even under wet-dry cycle conditions. In the future, this model is expected to be used to quantitatively evaluate the effects of internal moisture conditions on various material deterioration processes.

The authors thank Dr. Satoshi Tsuchiya from the COMS Engineering Corporation and Mr. Kazuhiro Tsuchiya, Mr. Tsubasa Abe, and Mr. Ken-ichi Kuribayashi for their valuable advice on the experimental and simulation processes used in this study.

References

1. M. Ohno, P. Limtong, and T. Ishida, Journal of Building Engineering **47**, (2022)
2. X. Ji, Y. Takahashi, T. Maeshima, I. Iwaki, and K. Maekawa, Structure and Infrastructure Engineering **18**, 1542 (2022)
3. F. Gong, S. Jacobsen, P. Li, Z. Wang, K. Maekawa, and M. Koniorczyk, Journal of Building Engineering **57**, (2022)
4. X. Pan, Z. Shi, C. Shi, T. C. Ling, and N. Li, Constr Build Mater **132**, 578 (2017)
5. X. Pan, Z. Shi, C. Shi, T. C. Ling, and N. Li, Constr Build Mater **133**, 81 (2017)
6. Z. Liu and W. Hansen, Cem Concr Compos **69**, 49 (2016)
7. K. Maekawa, T. Ishida, and T. Kishi, *Multiscale Modeling of Concrete Performance* (Taylor & Francis, 2008)
8. Japan Society of Civil Engineers, *Concrete Library 119, Recommendation for Concrete Repair and Surface Protection of Concrete Structures* (2005)
9. T. Konno, A. Hosoda, K. Kobayashi, and Y. Matsuda, Proceedings of JCI **29**, 541 (2007)
10. P. O'Neill Iqbal and T. Ishida, Cem Concr Res **39**, 329 (2009)
11. B. Liu, J. Qin, and M. Sun, KSCE Journal of Civil Engineering **23**, 3443 (2019)